# History-driven modulations of population codes in early visual cortex during visual search

Kirsten C.S. Adam[1,2] & John T. Serences[1,2,3]

[1] Department of Psychology, *University of California San Diego*
[2] Institute for Neural Computation, *University of California San Diego*
[3] Neurosciences Graduate Program, *University of California San Diego*

**Word count (abstract):** 149
**Word count (less abstract, methods, references, figure legends):** 4,007
**Word count (methods):** 2,215
**Tables:** 0
**Figures:** 7

**Keywords:** visual search; fMRI; priority maps; attentional selection; salience

**Contributions:** K.A. collected data, performed analyses, and drafted the manuscript. Both authors designed the study and revised the manuscript.

**Funding:** Research was supported by National Eye Institute grant R01 EY025872 (J.S.). and National Institute of Mental Health grant 5T32-MH020002 (K.A.).

**Data availability:** Data will be made freely available online on the Open Science Framework at https://osf.io/wrdvz/ upon acceptance for publication.

**Acknowledgements:** We thank Rosanne Rademaker for scanning assistance and for sharing custom analysis code. We thank Nicole Rangan and Matteo d'Amico for assistance with behavioral data collection, and we thank Ed Awh for helpful comments on the manuscript.

**Conflicts of interest:** none

**Correspondence to:**
Kirsten C. S. Adam
University of California San Diego
9500 Gilman Drive, Mail Code: 0109
La Jolla, CA 92093-0109
kadam@ucsd.edu

**Abstract**

To find important objects, we must focus on our goals, ignore distractions, and take our changing environment into account. This is formalized in models of visual search whereby goal-driven, stimulus-driven and history-driven factors are integrated into a priority map that guides attention. History is invoked to explain behavioral effects that are neither wholly goal-driven nor stimulus-driven, but whether history likewise alters goal-driven and/or stimulus-driven signatures of neural priority is unknown. We measured fMRI responses in human visual cortex during a visual search task where trial history was manipulated (colors switched unpredictably or repeated). History had a near-constant impact on responses to singleton distractors, but not targets, from V1 through parietal cortex. In contrast, history-independent target enhancement was absent in V1 but increased across regions. Our data suggest that history does not alter goal-driven search templates, but rather modulates canonically stimulus-driven sensory responses to create a temporally-integrated representation of priority.

## Introduction

At any moment we can selectively attend only a small fraction of available perceptual inputs due to a limited processing capacity, and the world around us is constantly changing. When performing visual search, we thus need to enhance relevant information, discard irrelevant information, and keep track of our changing surroundings. For example, when searching for sea glass at the beach, irrelevant but salient information (e.g., a red plastic bottle-cap) may grab our attention. But, if we repeatedly encounter the same irrelevant information (e.g., the beach is littered with red bottle-caps), then we can learn to ignore initially salient distractors.

Models of visual search hypothesize that we integrate information about what is relevant *(goal-driven* or *'top-down' factors*), what is salient given local image statistics *(stimulus-driven* or *'bottom-up' factors*), and what has occurred in the past (*history-driven factors*) via an integrated, topographically organized "priority map"[1–6]. Note, some work uses the terms 'saliency' and 'priority' interchangeably, whereas other work uses these terms to refer to distinct concepts. Here, we use 'priority' to refer to the integration of goal-driven and stimulus-driven task factors, and 'saliency' to refer to strictly to image-computable, stimulus-driven task factors[4].

Although both stimulus-driven and goal-driven information is represented to some extent in many cortical regions[4,7–11], areas of parietal cortex (e.g., LIP, IPS) are hypothesized to be ideal candidates for integrating information about stimulus-driven sensory inputs from occipital cortex and information about goals from pre-frontal cortex[12–15]. In contrast to goal-driven and stimulus-driven effects, history-driven effects have only recently been added to models of visual search, in part because these effects do not wholly fit within a 'goal-driven' versus 'stimulus-driven' dichotomous framework[1,16–18]. Rather, history-driven effects apparently rely upon the relationship between the current sensory input and knowledge of prior experiences. Much work has demonstrated how canonically 'goal-driven' and 'stimulus-driven' task manipulations alter neural activity in occipital and parietal cortex (i.e., selective attention[7,10,11,19–25] and stimulus-driven salience maps[3,26,27], respectively), but an open question is whether stimulus history influences attentional priority by co-opting elements of these computations.

Some accounts of history-driven effects predict that we exploit existing goal-driven selection mechanisms to incorporate information about history-driven task factors into priority maps. For example, when looking for a particular target, one may form a "template" of that feature and use this template to voluntarily up-regulate relevant portions of the visual field by co-opting goal-driven selective attention[28–33]. Thus, one possibility is that history-driven effects (e.g., repetition of target color) may strengthen the target template, and this increased goal-driven guidance would result in greater activation of the target position in a priority map. Likewise, if a particular distractor feature is repeated, one may form an analogous "negative template" for ignoring this feature[34–37] (but see[38,39]). However, not all evidence supports the notion that history-driven effects can be implemented via goal-driven selective attention[40–44]. Rather, integrating history into priority may exploit canonically 'stimulus-driven' mechanisms that are encapsulated within local sensory circuits (e.g., modulation of stimulus-driven saliency maps via adaptation[45,46], habituation[42–44] and/or repetition suppression[47,48]). Of course, these possibilities are not mutually exclusive. For example, distractor and target processing seem to be differentially affected by history[49–52]. Therefore, it may be that history-driven changes to priority are reflected in a combination of traditionally 'goal-driven' and 'stimulus-driven' neural signatures of priority. Alternatively, history-driven effects may also be coded via another pathway, such as via implicit and/or explicit learning of regularities within the medial-temporal lobe[13,53,54].

To test how stimulus history modulates priority, we measured neural activity via fMRI in human subjects performing a visual search task. If stimulus history influences search by altering the specificity of the goal-driven target template, then we would expect to see an enhanced representation of the target item's position, and this effect should be most pronounced in regions that are also most influenced by goal-driven selective attention such as IPS0. However, if stimulus history influences search by influencing canonically stimulus-driven sensory activity, then we would expect to see a decreased representation of the salient distractor's position, and this effect should be pronounced in areas most influenced by stimulus-driven salience such as V1. We thus estimated the strength of target and distractor representations in a 4-item search array across

retinotopically-defined visual cortical regions. Critically, we manipulated trial history such that we could compare neural responses to physically identical displays (e.g., green target, red singleton distractor) as a function of trial history (i.e., whether the colors of preceding displays repeated or varied).

To preview the results, we found that trial history modulated model-based estimates of distractor suppression, but not target enhancement, in retinotopically-defined visual areas. Furthermore, we found that visual regions were differentially modulated by goal-driven target enhancement and by history-driven distractor suppression. Whereas goal-driven modulations to population codes (i.e., target enhancement) were absent in V1 and were amplified across the visual hierarchy, history-driven effects were robust in V1 and across all other examined ROIs. Overall, the data suggest a dissociation between canonical 'goal-driven' mechanisms of attentional priority and 'history-driven' effects on distractor processing. We discuss our findings in the context of 'stimulus-driven' saliency models of V1, whereby history-driven task factors may directly modify priority within canonically stimulus-driven saliency maps, which integrate neural activity across trials as well as within a given trial, without the need for a 'goal-driven' template of the incidentally repeated information.

## Results

### Behavior

Subjects performed a variant of the additional singleton search task[55] (Figure 1A) in which they searched for a target (diamond) among non-targets (circles). On each trial, the participant reported via button-press the orientation of the line inside the diamond target (vertical or horizontal). On 66.67% of trials, one of the non-targets was uniquely colored ("singleton distractor present", e.g., one red distractor, two green non-targets, and one green target item). Behavioral capture was quantified as slowed response times (RTs) when the distractor was present versus absent. In addition to examining the basic capture effect, a key goal of this work was to examine modulation of capture by trial history[56–58]. Prior work has shown that participants can learn to suppress a distractor (i.e., no RT difference for singleton distractor present versus absent trials) when the same distractor color or distractor location is repeated over many trials[56–58]. Building on this

work, we included two key task conditions in a counterbalanced, block-wise fashion to manipulate trial history and behavioral capture while using identical stimulus arrays (e.g., green target, red distractor). In the color constant condition (Figure 1A), the array colors stayed constant throughout the block (e.g., green target, green non-target items, red distractor). In the color variable condition (Figure 1B), the array colors randomly varied from trial to trial. Based on prior work, we expected robust capture in the color variable condition, and little or no capture in the color constant condition[56–58].

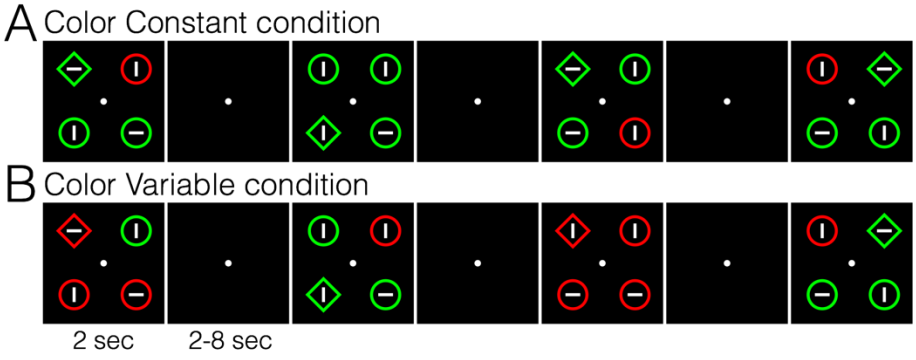


**Figure 1. Visual search task stimuli.** On each trial, participants viewed a 4-item array and reported the orientation of the line inside the diamond-shaped target (horizontal or vertical). **(A)** In the color constant condition, colors of targets and singleton distractors were fixed throughout the run. **(B)** In the color variable condition, colors of targets and singleton distractors swapped randomly from trial to trial.

Replicating prior work, we found significant behavioral capture that was modulated by trial history[40,41,50,56–59]. In our MRI sample (Exp 1a), we observed significant behavioral capture in the color variable condition, with longer RT's for distractor present versus distractor absent trials ($M$ = 32.8 ms, $SD$ = 25.5 ms, $p$ = .001, $d$ = 1.28), but capture was not significant in the color constant condition ($M$ = 10.8 ms, $SD$ = 18.5 ms, $p$ = .07, $d$ = .59). Importantly, capture was significantly larger for color variable vs. color constant runs ($p$ = .009, $d$ = .91). We replicated this pattern of findings in the behavior-only experiment (Exp. 1b), with robust capture for 'color variable' ($p < 1 \times 10^{-5}$, $d$ = 1.31), no significant capture for 'color constant' ($p$ = .1, $d$ = .32), and larger capture for color variable vs. constant ($p$ = .002, $d$ = .71). Participants in both experiments were accurate overall (>90%), and there was no evidence of a speed-accuracy trade-off (Analysis S1).

In addition to the key modulation of capture as a function of stimulus history, we also replicated prior findings that the degree of capture is significantly modulated by the physical distance between the target and the distractor[41,49,60,61], with larger capture for distractors nearer the target (Figure 2E-F). We ran a repeated measures ANOVA including both experiments (n=36). Including Experiment as a factor revealed no experiment main effects or interactions ($p > .2$), so the two experiments were combined for further analyses of the behavioral data (although Figure 2 shows data from the two experiments separately). There was a significant effect of Condition (larger capture for color variable than color constant), $p < 1x10^{-4}$, a main effect of Distance (larger capture for 90° than 180°), $p = .037$, $\eta^2_p = .12$, and an interaction between Condition and Distance (greater distance effect in the color variable condition), $p = .014$, $\eta^2_p = .16$.

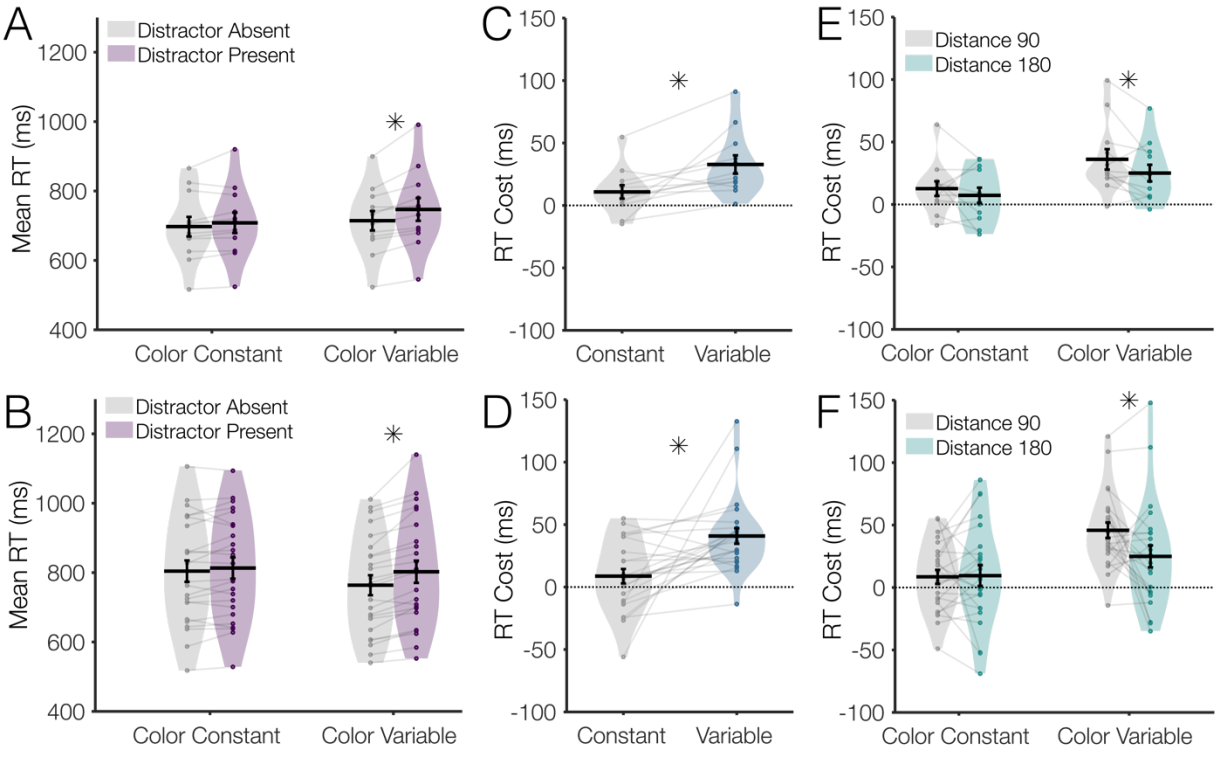


**Figure 2. Behavioral capture during the visual search task. (A)** In the main MRI Experiment (Exp 1a), participants were significantly captured by the salient singleton distractor in the color variable condition, but not in the color constant condition. **(B)** This pattern replicated in the behavior-only experiment (Exp 1b). **(C-D)** Capture costs (RT Difference for distractor present – absent trials) were significantly larger in the color variable than in the color constant condition in Exp 1a **(C)** and Exp 1b **(D)**. **(E-F)** Capture

costs (RT Difference for distractor present – absent trials) were significantly modulated by the distance between the target and distractor in the color variable condition both in Exp 1a **(E)** and Exp 1b **(F)**. Violin plot shading shows range and distribution of the data; dots represent single subjects; black error bars indicate ±1 SEM.

**fMRI results: Model estimates of spatial position in the independent mapping task**

We opted for a multivariate model-based approach to estimate the amount of information encoded in voxel activation patterns about each of the 4 stimuli in the search array, as such multivariate approaches are more sensitive than just computing the univariate mean response across all voxels[62–67]. For example, item-specific information has been observed using multivariate methods even in the absence of univariate changes[68,69] (but for univariate analyses of the present data, see Figure S1). We opted for an inverted encoding model (IEM) approach[70,71], as opposed to Bayesian or other decoders[72,73], because this approach allowed us to easily derive a separate estimate of the information encoded about each of the 4 simultaneously presented items from the search array in the main analysis[70].

In our key analyses of the fMRI data, we used an independent mapping task to train a model of spatial position from which we estimated the relative priority of all item positions within the visual search array. During the independent mapping task, observers viewed a flickering checkerboard wedge that was presented at 1 of 24 positions on an imaginary circle around fixation (Figure 3A). We first checked that we observed robust estimates of spatial position when training and testing within the independent mapping task (leave 1 run out, see section 'Inverted Encoding Model'). We observed robust model-based estimates of spatial position for all ROIs (Figure 3B). Parameters from the best-fitting von Mises distribution to each region-of-interest (ROI) are depicted in Figure 3C (model fits are shown in Figure S2). There was an effect of ROI on precision such that spatial position was represented less precisely in later visual areas ($p < 1x10^{-5}$, where precision is the concentration parameter κ of the best fitting von Mises, with higher values indicating a more precise function). There was also an effect of ROI on the amplitude and baseline measures of the model-based estimates of spatial position ($p < 1x10^{-5}$), and all 3 parameters significantly differed from zero across all ROIs ($p < 1x10^{-5}$). These results,

particularly the observation of amplitudes greater than 0, confirmed that activation patterns in all examined regions encode information about spatial position.

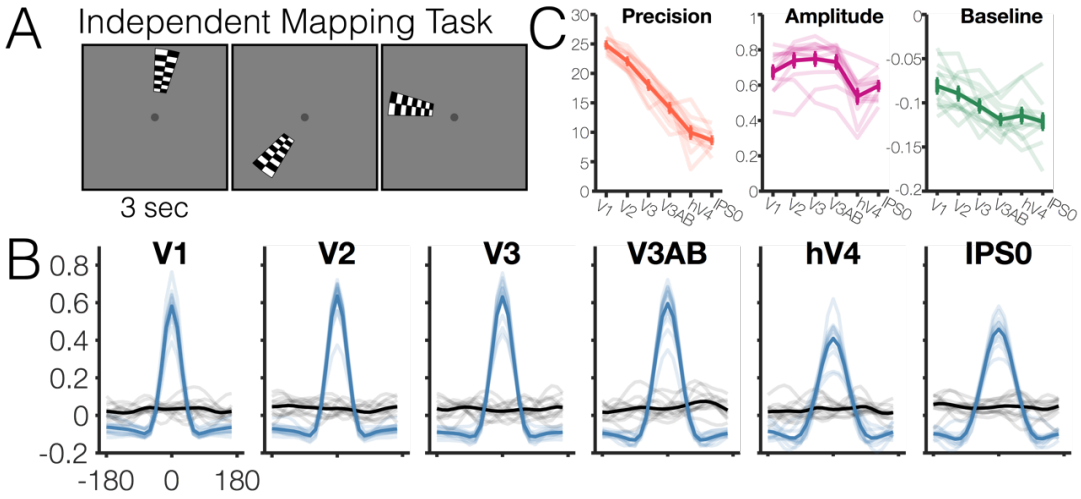


**Figure 3. Single-item model estimates training and testing within the independent mapping task. (A)** Independent mapping task used to train the model to estimate spatial position of 4 search array items. Participants viewed a flickering checkerboard which could appear at one of 24 positions around an imaginary circle. **(B)** Blue lines: Model estimates of viewed spatial position training and testing within the independent mapping task. Single-trial model estimates for each subject are aligned to 0 degrees and averaged. Black lines: Model estimates for shuffled training labels. Opaque lines = group average; semi-transparent lines = individual subjects. **(C)** Descriptive statistics for best fit von Mises parameters (precision [κ], amplitude, baseline) to model estimates in panel B. Error bars indicate ±1 SEM; the opaque line shows the group average; semi-transparent lines show individual subjects.

Unlike the single item model estimates that were derived based on the independent mapping task (Figure 3), we could not fit a simple, uni-modal Gaussian function to model-based estimates derived from the search task data because 4 peaks in the model output were expected – one for each item in the search array. As such, we first conducted simulations to ensure that we would be able to measure putative changes to individual item representations (e.g. target enhancement, distractor suppression), despite multiple item representations contributing to the aggregate 4-item model estimates. To do so, we used data from the independent mapping task to generate predictions for observed model responses in a 4-item array. For each ROI, we took the 1-item model

response derived from the independent mapping task, replicated this model response four times (once at each of the four search array positions), and took the average of all 4 shifted 1-item model response lines to generate a single 4-item model prediction. In addition, we systematically varied the strength of the simulated response to each item to ensure that we were able to recover a corresponding change in the item-specific responses estimated from the aggregate 4-item model estimate (Figure 4; Figure S3).

These simulations revealed clearly separable peaks for all four items in early areas like V1, where spatial precision is high (Figure 4A-B, left panel). In contrast, identifying clear peaks in later areas like IPS0 was difficult when the response to all items was equivalent (Figure 4A-B, right panel). However, if one item evoked a larger or smaller response than the other items, as would be expected with target enhancement or distractor suppression, then clear and measurable changes to the aggregate 4-item model estimates emerged (Figure 4C). Further simulations showed that we could detect smaller changes to one item (e.g., distractor suppression) in the presence of larger changes to another item (e.g., target) by measuring the response amplitude at each expected item's peak. In V1, this is clearly seen in the peak response to each item; in later areas such as IPS0, such changes manifest as a large central peak that is skewed by the neighboring items' smaller changes (Figure 4D).

We also used a general linear model (GLM) to estimate best-fitting gain factors for each of the 4 hypothesized item representations by fitting an aggregate function and allowing one parameter in the GLM to scale the response associated with each item. This is essentially the inverse of the simulations described above: For a given aggregate response (i.e., the response of each of the 24 spatial channels when shown a given 4-item search array), we used a non-negative least squares solution[74] to estimate the contribution of each of the 4 item positions (calculated from the 1-item localizer task) to the observed 4-item search array response (Figure 4E). This analysis yielded similar results to the simple approach of comparing the height at each expected item peak (e.g., Analysis S2-4). Thus, using either the raw amplitude at expected peaks or a GLM-based approach, we determined that we should be able to accurately characterize situations in

which there was no modulation of target and distractor responses as well as situations in which there was a significant modulation of target and/or distractor responses.

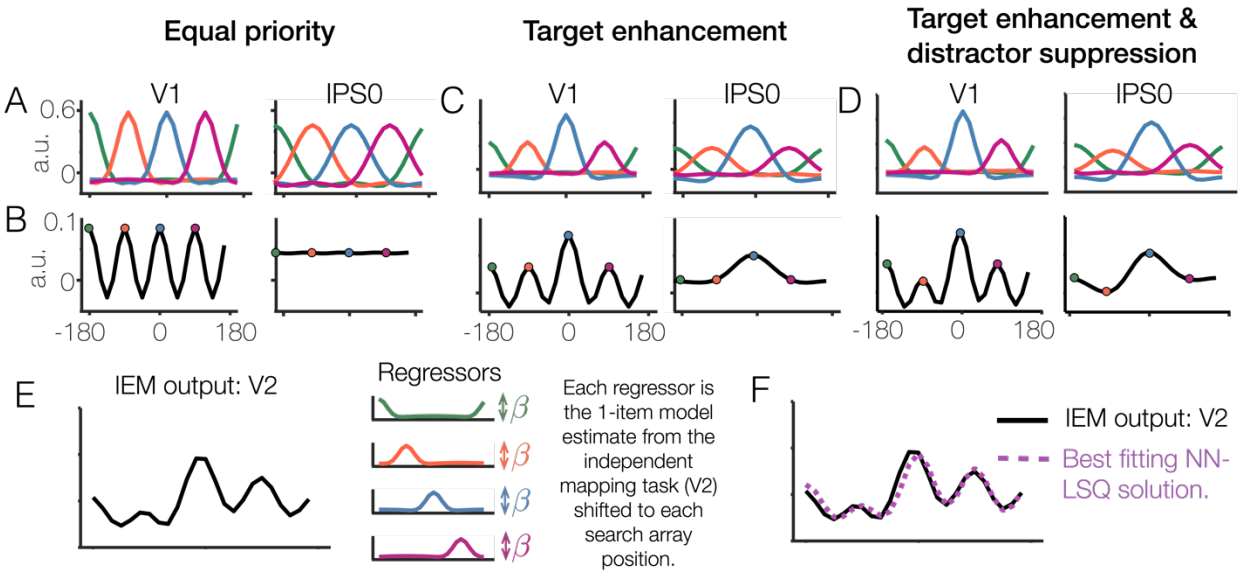


**Figure 4. Generating predictions for 4-item model estimates by averaging single-item model estimates from the independent mapping task. (A)** Average from the independent mapping task plotted at 4 hypothetical item locations. Here, these 4 "items" are represented with equal priority. (B) Hypothetical observed response when measuring a single trial containing the 4 items presented simultaneously. This line is the average of all lines in Panel A. (C) The same as panels A and B, but with the item at position 0 assigned a higher response amplitude than the other three items. (D) The same panels as A and B, but with both an enhanced item at position 0 and a suppressed item at position -90. (E) Actual IEM model output for 4-item search arrays in V2 (Target plotted at 0, distractor plotted at -90). To estimate the strength of each of the 4 underlying item representations, one can simply measure the height (a.u.) at expected item peaks (i.e., -180, -90, 0, and 90). Alternatively, one may use a non-negative least squares solution to estimate weights for a regressor for each of the 4 item positions. Each regressor is the 1-item IEM output from the independent mapping task within the same region (e.g., V2), shifted to the appropriate item location. (F) Example IEM output and best-fitting non-negative least squares solution with 4 item regressors.

**Analysis of search array locations in V1, V2, V3, V3AB, hV4, and IPS0.**

Given that we can assess differential responses associated with each of the 4 items in the search array (Figure 4), we next tested whether goal- and history-driven modulations were differentially represented across the visual stream by performing an analysis of history-driven effects on target and distractor processing across visual ROIs

(Figure 5). These six ROIs (V1, V2, V3, V3AB, hV4 and IPS0) were chosen for each participant having at least 90 spatially selective voxels as determined by the localizer data. Here, we focus on history-driven effects on target processing and distractor processing for the arrays where behavioral and neural distractor competition effects were greatest (target-distractor separation +/-90°, see Figure 2E,F). Full ANOVA results and additional plots are shown for individuals ROIs with both array 90° and 180° configurations in Figure S7-8 and Analysis S5.

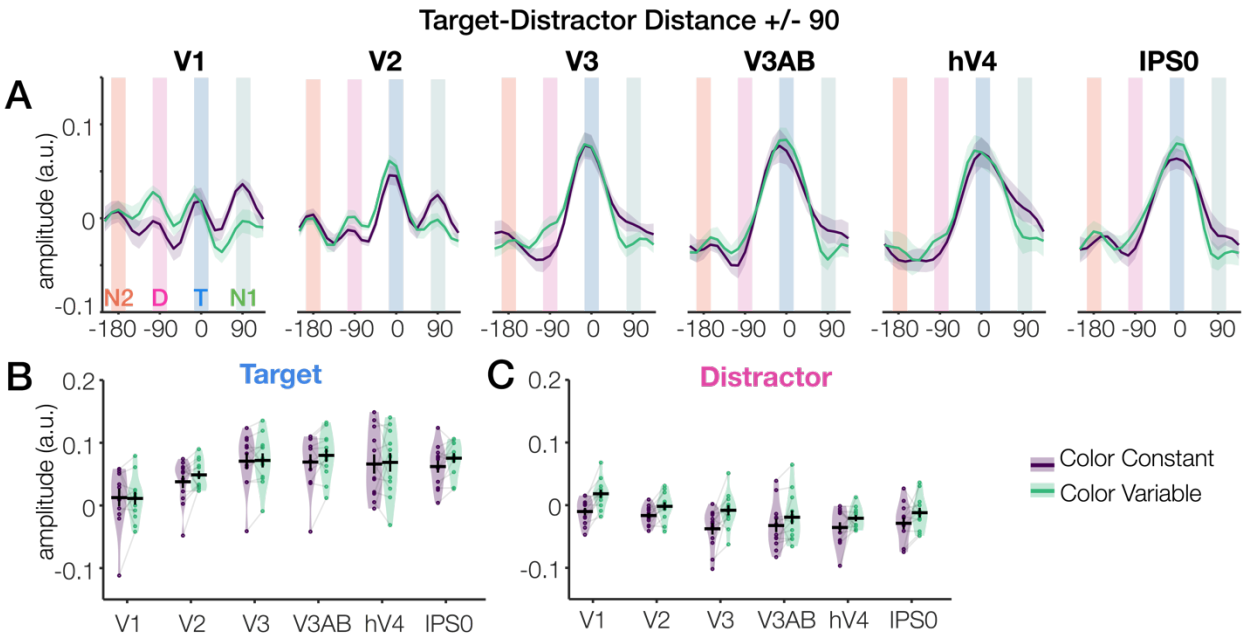


**Figure 5. Dissociable effects of stimulus history on target enhancement and distractor suppression.** (A) Model responses for individual ROIs as a function of task condition (Arrays with target-distractor distance +/-90). Purple and green lines (Shaded error bars = 1 SEM) show the output of the inverted encoding model in the color constant and color variable conditions, respectively. Target enhancement can be seen as the greater height at position 0; history-driven distractor suppression can be seen as the lower height at position -90 for the purple vs. green line. Background panels at -180°, -90°, 0° and +90° show the positions of the 4 search array items (blue = target (T), pink = distractor (D), green = non-target 1(N1), orange = non-target 2 (N2), (B) Target amplitude as a function of ROI and task condition. There was no effect of task condition on target amplitude, but a significant increase in target amplitude across ROIs. Violin plot shading shows range and distribution of the data; dots represent single subjects; black error bars indicate ±1 SEM. (C) Distractor amplitude as a function of ROI and task condition. There was a significant effect of task condition on distractor amplitude, and this history-driven effect did not interact with ROI.

We found evidence for within-display target enhancement (i.e., enhancement of the target over other positions), but we did not find evidence for history-driven modulations of target enhancement. Overall target enhancement was significant in all ROIs (all $p$'s < .001) except for V1 ($p$'s > .12), and target enhancement significantly increased across ROIs ($p$ < .001) as shown in Figure 6A-B. There was, however, no meaningful effect of history on target amplitude as revealed by a repeated-measures ANOVA testing the main effect of history and the interaction between history and ROI on target processing ($p$ = .35, $\eta^2_p$ = .08; $p$ = .64, $\eta^2_p$ = .04 for main effect and interaction respectively). This pattern was the same whether we used raw amplitude values or we used values from the GLM (no effect of history, $p$ = .28, no interaction of history and ROI, $p$ = .51).

In contrast, history had a significant effect on distractor amplitude such that distractor amplitudes were significantly attenuated in the color constant condition relative to the color variable condition. A repeated-measures ANOVA revealed a main effect of history ($p$ = .007, $\eta^2_p$ = .50) and no interaction between history and ROI ($p$ = .44, $\eta^2_p$ = .08), indicating that the effect of history on distractor processing was similar throughout the examined ROIs. Though the ANOVA suggests that history effects were of a similar magnitude across all examined ROIs, a post-hoc simple main effects analysis showed that the effect was individually significant only in V1 ($p$ < .001) and V3 ($p$ < .01). This general pattern was the same whether we used raw amplitude values or else used values from the GLM approach (main effect of history, $p$ = .01, $\eta^2_p$ = .47, no interaction of history and ROI, $p$ = .87, $\eta^2_p$ = .03).

Finally, we examined changes in non-target responses. For "non-target 1" (the item neighboring the target on the side opposite the distractor), there was an overall history related modulation (color constant > color variable, $p$ = .016, $\eta^2_p$ = .42) that did not interact with ROI ($p$ = .76, $\eta^2_p$ = .03). Similar general effects on non-target processing have been observed recently[51] and may reflect a bias of attention away from the distractor such that attention may 'overshoot' the target because of the reduction in signal at the distractor location. The effect of history on "non-target 1" responses likewise was similar though of

borderline significance in the GLM analysis (color constant > color variable, $p = .049$, $\eta^2_p = .31$). We found no effect of history on the other non-target ("non-target 2") which occupied the spatial position 180 degrees from the target item ($p >= .61$).

Finally, additional analyses on larger, aggregate ROIs (V1-V3, IPS0-3) yield convergent results and also demonstrate how distractor suppression effects were absent for arrays where the target and distractor did not compete with each other (target-distractor separation +/- 180°), consistent with our separate analysis of each ROI (Figure 6) and prior behavioral and neural findings[41,49,51,60] (Analysis S2-4, Figures S4-6).

## Discussion

To find what we are looking for, we must integrate information about stimulus relevance, salience, and history. While the impact of stimulus relevance and salience on topographically organized population codes have been thoroughly investigated, stimulus history is not thought to be a wholly goal-driven or stimulus-driven process as history effects depend on interactions between the current stimulus drive ('bottom-up' factor) and the current internal state of the visual system ('top-down' factor). To address this ambiguity and to better understand how history impacts visual processing, we tested whether history-driven changes to attentional priority operate in a manner akin to canonically goal-driven and/or to stimulus-driven signatures of priority. To do so, we estimated population-level neural responses evoked by 4-item search arrays across retinotopically-defined areas of occipital and parietal cortex. We found that stimulus history did not modulate the specificity of goal-driven target templates, as goal-driven target enhancement was unaffected by stimulus history. Instead, we found that stimulus history attenuated responses related to distractors throughout the visual hierarchy. These results suggest that stimulus history may influence visual search performance via local competitive interactions within early sensory cortex (i.e., V1).

Traditional models of image-computable salience propose that local image statistics determine competitive interactions that give rise to 2D spatial salience maps within V1[26,27], and these models do not typically account for the effects of stimulus history. However, recent work suggests that neural adaptation – which is linked to the history of

prior stimuli – in a subset of tuned neurons may alter stimulus-driven competitive dynamics (e.g., divisive normalization[75]) within early visual cortex[76]. Thus, to accommodate our observation of history-driven distractor suppression within existing saliency models, we propose that stimulus-driven evoked responses may be integrated over a longer, multi-trial duration (as opposed to just within a single image; Figure 6)[77–79]. In the context of models of visual search, this might be comprised of a series of 2D spatial maps that together form a temporally integrated 3D salience map (i.e., salience is computed based on current and prior physical stimulus properties). Consistent with the notion of a 3D salience map, recent behavioral and neural evidence suggests a role for priming and habituation in visual search behaviors[42–44,50,80] (also see[81]).

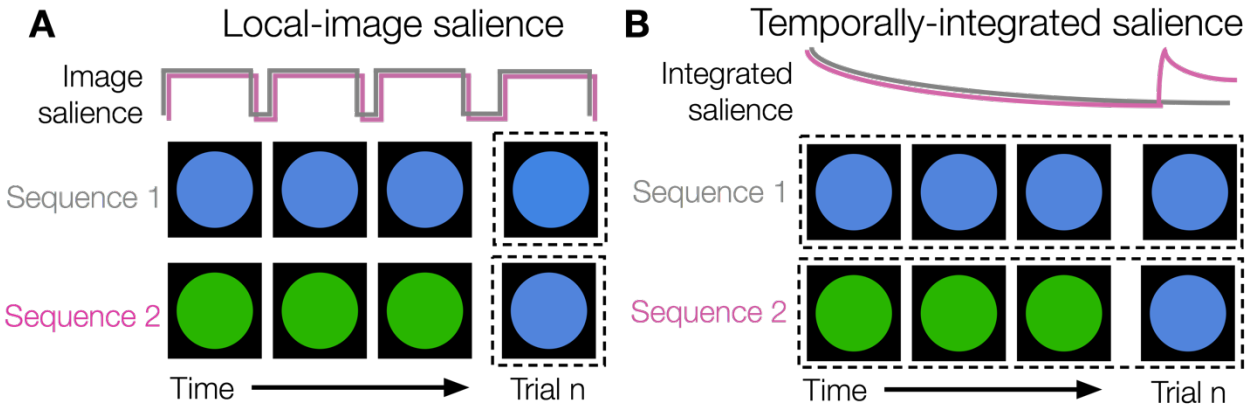


**Figure 6. Simplified cartoon illustration of local-image versus temporal-integration salience for a simple image with one feature and location.** (A) In 2-D salience computations, stimulus-driven stimulus drive is determined locally within a given image without respect to prior images. Sequence 1 is 4 different trials, and on each trial the same stimulus is shown (Blue-Blue-Blue-Blue). Sequence 2 is 4 different trials, but the final trial is a different color from the preceding trials (Green-Green-Green-Blue). The final trial (Blue) is physically identical for the two sequences. So, the final stimuli (trial n in each sequence) have identical 2-D salience. Assuming that we chose equiluminant green and blue values, then each "frame" in the sequence likewise has approximately the same image-computable salience, as shown by the uniform-sized square pulses in the cartoon. (B) Alternatively, stimulus-driven salience maps may better be conceived of as reflecting a temporally-integrated 3-D salience map, as early sensory neurons adapt to ongoing stimulus features. In Sequence 1 (Blue-Blue-Blue-Blue), the activity of neurons that are maximally responsive to blue wanes due to adaptation. In Sequence 2 the activity of neurons maximally responsive to green wanes over the first 3 trials, but the final stimulus elicits a robust response from the non-adapted blue-preferring neurons. Thus, temporally-integrated salience for the trial *n* in each sequence differs across the two sequences even though the stimuli are physically identical.

Consistent with a temporally-integrated salience account of history-driven distractor suppression, we observed history-driven modulations only with sufficient competition (i.e., targets and distractors were closer together) and we observed robust history-driven modulations in V1 in the absence of goal-driven modulations. In line with our findings, prior behavioral work has shown that incidental repetitions of distractor, but not target, features and locations modulate search performance[49,50]. Likewise, prior work has shown a rapid suppression of distractor-evoked neural responses[56,57,82–86] and that the likelihood of distraction results in anticipatory changes to distractor, but not target, locations[51,87,88]. However, the proposed temporally-integrated salience account does not capture all history-driven effects. In our task, the repeated distractor features were purely visual in nature, and thus history effects might be mediated entirely via local circuit dynamics (i.e., the adaptation account described above). In contrast, other studies have examined history-driven effects for more abstract features like reward[10,19,89–95] (but also see[96,97]), which may require an intermediary pathway such as the medial-temporal lobe[13] or dopaminergic midbrain structures[89,98].

In addition to implicating early visual cortex in representing history-driven task factors during visual search, we also replicated prior findings that the locations of attended items (here, search targets) are prioritized relative to other item locations in both visual and parietal cortex[7,8,10]. These target-related modulations are consistent with the broad involvement of visually-responsive regions in representing goal-driven priority during visual search[19,25]. For example, recent studies manipulated the salience (contrast) and relevance (attended or unattended) of items and found that salience and relevance were both represented, to varying degrees, across the visual hierarchy[8,20]. Notably, however, here we found that target prioritization was absent in V1, whereas prior work has found robust effects of attention in V1[7,10,11,21–24,99,100]. This difference may reflect task differences — much prior work found attention-related gains in V1 when spatial attention was cued in advance or a single target was shown, whereas visual search arrays provide visual drive at many competing locations and spatial attention is deployed only after array onset. In addition, our work suggests that further work may be needed to unconfound history effects and attention effects in the study of spatial attention, as much early work

448 on univariate attention effects has employed blocked designs where the same location is
449 attended for many trials in a row[21,22,24,99,100].

450 Although our work suggests that stimulus history modulates representations of
451 distractor but not target processing in visual cortex, there are some potential limitations
452 to the current design that suggest avenues for future work. First, because we measured
453 only location, we could not directly measure suppression of the distractor color[40].
454 However, as the spatial position of the distractor was completely unpredictable, our
455 results do strongly imply that the distractor color was suppressed. Likewise, most theories
456 of visual search hypothesize that space is the critical binding medium through which
457 feature and goal maps are integrated[3,5,6], and recent work suggests that location is
458 spontaneously encoded even when only non-spatial features such as color are task-
459 relevant[101]. Second, it is possible that history may modulate both distractor- and target-
460 processing in other circumstances not tested here. That is, perhaps the target template
461 'diamond' in our task was sufficiently useful such that adding feature information to this
462 template (e.g., 'red diamond' rather than 'diamond') did not confer a behavioral advantage
463 (but see[102]). Finally, the time-course of MRI (sampling every 800 ms) is slower than shifts
464 of spatial attention to the search target (< 500 ms)[103]. Although the history-driven effects
465 that we observed in visual cortex are consistent with the rapid distractor suppression
466 effects observed in EEG[82,83], we cannot definitively say on the basis of these data that
467 the observed history-driven effects occurred rapidly and directly within visual cortex
468 versus via recurrent feedback from later visual areas. Nonetheless, the present work is
469 consistent with and provides critical initial evidence for such a model.
470
471 **Methods**
472 **Participants**
473 **Experiment 1a: MRI experiment.** Healthy volunteers ($n$ = 12; 9 female; mean age
474 = 25.3 years [SD = 2.5, min = 21, max = 30]; all right-handed; normal or corrected-to-
475 normal visual acuity; normal color vision) participated in three ~2 hour sessions at the
476 Keck Center for fMRI on the University of California San Diego (UCSD) campus, and were
477 compensated $20/hr. Procedures were approved by the UCSD Institutional Review

Board, and participants provided written informed consent. Sample size was determined by a power analysis on data from Sprague et al.[8] where achieved power (1-ß) to detect a within-subjects attention modulation using an inverted encoding model was 83% (across 10 ROIs) with n=8. We planned for n =11 to achieve estimated 90% power (rounded up to n = 12 to satisfy our counter-balancing criteria).

**Experiment 1b: Behavior only.** Healthy volunteers (*n* = 24; 21 female; mean age = 19.8 years [SD = 1.5, min = 18, max = 24]; normal or corrected-to-normal visual acuity; normal color vision; handedness not recorded) participated in one 1.5-hour experimental session in the Department of Psychology on the UCSD campus, and were compensated with course credit. Procedures were approved by the UCSD IRB, and all participants provided written informed consent. A sample size of 24 was chosen *a priori* based on published papers[56].

## Session procedures

**Exp 1a, Retinotopy session.** Participants completed one retinotopic mapping session prior to participation in the experimental sessions, following standard procedures[104,105]. Some participants had already completed a retinotopy session as part of prior studies in the lab; this session was used if available. Retinotopy data were used to identify retinotopic ROIs (V1-V3, V3AB, hV4, VO1, VO2, LO1, LO2, TO1, TO2, IPS0-4). During each session, participants viewed flickering checkerboards. On meridian mapping runs, a “bowtie” checkerboard alternated between the horizontal and vertical meridians. On polar angle mapping runs, a checkerboard wedge slowly rotated in a clockwise or counterclockwise direction. On eccentricity mapping runs, a “donut” checkerboard began near fixation and its radius slowly expanded outward. A high-resolution anatomical scan was collected for functional alignment. Anatomical and functional retinotopy analyses were performed using custom code caling existing FreeSurfer and FSL functions. Functional retinotopy data were used to draw ROIs, but only voxels that were also visually responsive to experimental localizers (below) were analyzed further.

**Exp 1a, Main MRI session.** Participants completed two experimental sessions. In each session, they completed 2 runs of the item position localizer, 4 runs of the spatial location localizer, and 8 runs of the search task (4 runs "color variable", 4 runs "color constant"). When time allowed, extra localizer runs were collected. Some participants also took part in an unrelated study in which additional localizers were collected.

**Exp 1b.** Participants completed 12 blocks of the search task (6 blocks "color variable", 6 blocks "color constant").

## Stimuli and task procedures

### Experiment 1a: MRI

Stimuli were projected on a 21.5 x 16 cm screen mounted inside the scanner bore. The screen was viewed from a distance of ~47 cm through a mirror. Stimuli were generated in MATLAB (2017b, The MathWorks, Natick, MA) with the Psychophysics toolbox [106,107] on a laptop running Ubuntu. Responses were collected with a 4-button button box. Stimuli for each task are shown in Figure 1.

**Item position localizer.** Participants viewed reversing checkerboards (4 Hz flicker) which occupied the locations of the items in the search task (each item radius = 2.5º placed on an imaginary circle 7º from fixation, with one item in each of the 4 quadrants on the circle). Participants were shown items on 2 alternating diagonals (i.e., items in Quadrants 1 and 3 and then Quadrants 2 and 4) for 3 sec each. There were 88 stimulus presentations within each run. Participants were instructed to attend to both items, and to press a button if either item briefly dimmed. A brief (250 ms) dimming occurred on 1 of the 2 items for 25% of stimulus presentations.

**Spatial location localizer.** Participants viewed a reversing checkerboard wedge (flicker = 4 Hz; white & black checkerboards) at one of 24 positions. Checkerboard positions were equally spaced along a circle with radius = 7º, and wedges were non-overlapping (i.e., each wedge's width along the circle filled a 15º arc and was ~5º of visual angle in height). The wedge stayed at one position for 3 sec, then moved to a different position (with the constraint that back-to-back positions must be in different quadrants). There were 96 wedge presentations within each run. Participants were instructed to

attend to the fixation point; if the fixation point's color changed (increase or decrease in brightness), they pressed a button on the button box. A total of 20 fixation point color changes occurred throughout each run; changes to the fixation cross happened at random times with respect to wedge stimulus onsets.

**Search task.** Participants performed a variant of the additional singleton search task (Theeuwes, 1992). On each trial, participants saw a search array containing 4 items (item colors were red, RGB = 255,0,0, or green, RGB = 0,255,0, and presented on a black background, RGB = 0,0,0). The items (2.4º radius) were placed on an imaginary circle 7º from fixation with 1 item in each visual quadrant (i.e., 45º, 135º, 225º & 315º). Participants fixated a small, gray dot (.2º) throughout each run. Participants searched for a "target" (the diamond-shaped item) among distractor items and reported the orientation of the small line inside (line size = .08º x .94º; orientation = horizontal or vertical) by pressing one of two buttons. Non-singleton distractors, 'non-targets', had the same color as the shape-defined target (e.g., green circles). A "singleton distractor" was present on 66.67% of trials, and was a color singleton (e.g., red circle). Stimuli are illustrated in Figure 1. Target location (quadrant 1-4), distractor location relative to the target (-90º, +90º, or +180º), distractor presence (66.67% present), and the orientation of the line inside the target (horizontal or vertical) were fully counterbalanced within each run, for a total of 72 trials per run. Search set size was held constant at 4 items. The search array was presented for 2 sec followed by a blank inter-trial interval (equal probability of 2, 3.2, 5, or 8 sec).

We manipulated the degree to which participants were behaviorally captured by the distractor by changing trial history. In "color variable" runs, the colors of targets and distractors swapped unpredictably. In "color constant" runs, the colors of targets and distractors were fixed throughout the run (e.g., the targets and non-singleton distractors were always green and the singleton distractor was always red). Based on prior work [57,58], we expected to observe robust behavioral capture by the singleton distractor in the color variable runs and no behavioral capture in the color constant runs.

Run types were blocked and partially counterbalanced within and across sessions, such that the order of the 2 conditions would be balanced across the 2 sessions for each

participant. For example, if in Session 1 a participant first received 4 color variable runs followed by 4 color constant runs (red), then in Session 2 they would first receive 4 color constant runs (green) followed by 4 color variable runs.

**Experiment 1b: Behavior**

Participants performed the same additional singleton search task described above. Participants viewed the stimuli on CRT monitors (39 x 29.5 cm) from a distance of ~52 cm. Stimulus parameters (size, color) and trial timing were matched to the fMRI experiment. Each experimental block contained a total of 48 search trials. Participants performed a total of 12 blocks of trials (6 color variable, 3 color constant with red targets, 3 color constant with green targets). The color constant and color variable conditions were blocked and counterbalanced across participants (half of participants received the color variable condition first).

**Magnetic resonance imaging acquisition parameters**

Scans were performed on a General Electric Discovery MR750 3.0T scanner at the Keck Center for Functional Magnetic Resonance Imaging on the UCSD campus. High-resolution (1mm$^3$ isotropic) anatomical images were collected as part of the retinotopy session. Most participants' (10 of 12) anatomical images were collected with an Invivo 8-channel head coil; 2 participants' anatomical images were collected with a Nova Medical 32-channel head coil (NMSC075-32-3GE-MR750). GE's "Phased array Uniformity Enhancement" (PURE) method was applied to anatomical data acquired using the 32-channel coil in an attempt to correct inhomogeneities in the signal intensity. Functional echo-planar imaging (EPI) data were collected with the Nova 32 channel coil using the GE multiband EPI sequence, using nine axial slices per band and a multiband factor of eight (total slices = 72; 2 mm$^3$ isotropic; 0 mm gap; matrix = 104 × 104; field of view = 20.8 cm; repetition time/echo time (TR/ TE) = 800/35 ms, flip angle = 52°; in-plane acceleration = 1). The initial 16 TRs in each run served as reference images for the transformation from *k*-space to image space. Un-aliasing and image reconstruction procedures were performed on local servers and on Amazon Web Service servers using

code adapted from the Stanford Center for Cognitive and Neurobiological Imaging (CNI). Forward and reverse phase-encoding directions were used during the acquisition of two short (17 sec) "top-up" datasets. From these images, susceptibility-induced off-resonance fields were estimated [108] and used to correct signal distortion inherent in EPI sequences, using FSL top-up [109,110].

**Pre-processing**

Pre-processing of imaging data closely followed published lab procedures[111] using FreeSurfer and FSL. We performed cortical surface gray-white matter volumetric segmentation of the high-resolution anatomical volume from the retinotopy session using FreeSurfer's "recon-all" procedures[112]. The first volume of the first functional run from each scanning session was coregistered to this common T1-weighted anatomical image. To align data from all sessions to the same functional space, we created transformation matrices with FreeSurfer's registration tools[113], and used these matrices to transform each four-dimensional functional volume using FSL's FLIRT[114,115]. After cross-session alignment, motion correction was performed using FSL's McFLIRT (no spatial smoothing, 12 degrees of freedom). Voxelwise signal time-series were normalized via Z-scoring on a run-by-run basis. Analyses after preprocessing were performed using custom scripts in MATLAB 2018A.

**fMRI analyses: Inverted encoding model**

**Voxel selection for Decoding ROIs.** We defined visual ROI's using data from the retinotopy session following published lab procedures[7,111]. From these retinotopically-derived ROI's, we chose the subset of voxels that were spatially selective for the stimuli used in this task. We thresholded voxels using the independent mapping task data. We ran a one-way ANOVA with factor Quadrant on each voxel; significant voxels ($p < .05$ uncorrected) were retained for analysis. For the aggregate analyses, we *a priori* created an early visual cortex ROI (all spatially selective voxels from V1-V3) and a parietal cortex ROI (all spatially selective voxels from IPS0-3). For individual ROI analyses, we used all

individual retinotopic ROIs for which there were a minimum of 90 spatially selective voxels per participant: V1, V2, V3, V3AB, hV4, and IPS0.

**Inverted Encoding Model.** Following prior work[7,116], we used an inverted encoding model to estimate spatially-selective tuning functions from multivariate, voxel-wise activity within each ROI. We assumed that each voxel's activity reflects the weighted sum of 24 spatially selective channels, each tuned for a different angular location. These information channels are assumed to reflect the activity of underlying neuronal populations tuned to each location. We modeled the response profile of each spatial channel as a half sinusoid raised to the 24th power:

$$\mathrm{R} = \sin(0.5\theta)^{24},$$

where $\theta$ is angular location (0–359°, centered on each of the 24 bins from the mapping task), and $R$ is the response of the spatial channel in arbitrary units.

Independent training data $B_1$ were used to estimate weights that approximate the relative contribution of the 24 spatial channels to the observed response at each voxel. Let $B_1$ ($m$ voxels × $n_1$ observations) be the activity at each voxel for each measurement in the training set, $C_1$ ($k$ channels × $n_1$ observations) be the predicted response of each spatial channel (determined by the basis functions) for each measurement, and $W$ ($m$ voxels × $k$ channels) be a weight matrix that characterizes a linear mapping from "channel space" to "voxel space". The relationship between $B_1$, $C_1$, and $W$ can be described by a general linear model:

$$\mathrm{B}_1 = \mathrm{W}\mathrm{C}_1$$

We obtained the weight matrix through least-squares estimation:

$$\widehat{\mathrm{W}} = \mathrm{B}_1{\mathrm{C}_1}^{\mathrm{T}}\left(\mathrm{C}_1{\mathrm{C}_1}^{\mathrm{T}}\right)^{-1}$$

In the test stage, we inverted the model to transform the observed test data $B_2$ ($m$ voxels × $n_2$ observations) into estimated channel responses, $C_2$ ($k$ channels × $n_2$ observations), using the estimated weight matrix, $\widehat{\mathrm{W}}$, that we obtained in the training phase:

$$\widehat{\mathrm{C}_2} = \left(\widehat{\mathrm{W}}^{\mathrm{T}}\widehat{\mathrm{W}}\right)^{-1}\widehat{\mathrm{W}}^{\mathrm{T}}\mathrm{B}_2$$

Each estimated channel response function was then circularly shifted to a common center by aligning the estimated channel responses to the channel tuned for target location.

**Model training and testing.** We trained the IEM using independent mapping task data and tested the model using single trial search-task data (average of 4 to 10 TR's after search array onset). We then shifted and averaged the search task data so that like trials were aligned (e.g., rotate and average all trials with target-distractor distance of 90). To reduce idiosyncrasies of only having 1 test set, we iterated the analysis by leaving out 1 block of training data and 1 block of test data, looping through all possible combinations (e.g., for each 1 block of left out training data, we left out each possible block of test data on different runs of the loop).

## References


1. Awh, E., Belopolsky, A. V. & Theeuwes, J. Top-down versus bottom-up attentional control: a failed theoretical dichotomy. *Trends in Cognitive Sciences* **16**, 437–443 (2012).
2. Fecteau, J. & Munoz, D. Salience, relevance, and firing: a priority map for target selection. *Trends in Cognitive Sciences* **10**, 382–390 (2006).
3. Itti, L. & Koch, C. A saliency-based search mechanism for overt and covert shifts of visual attention. *Vision Research* **40**, 1489–1506 (2000).
4. Serences, J. T. & Yantis, S. Selective visual attention and perceptual coherence. *Trends in Cognitive Sciences* **10**, 38–45 (2006).
5. Treisman, A. M. & Gelade, G. A feature-integration theory of attention. *Cognitive Psychology* **12**, 97–136 (1980).
6. Wolfe, J. M. Guided Search 2.0 A revised model of visual search. *Psychonomic Bulletin & Review* **1**, 202–238 (1994).
7. Sprague, T. C. & Serences, J. T. Attention modulates spatial priority maps in the human occipital, parietal and frontal cortices. *Nature Neuroscience* **16**, 1879–1887 (2013).
8. Sprague, T. C., Itthipuripat, S., Vo, V. A. & Serences, J. T. Dissociable signatures of visual salience and behavioral relevance across attentional priority maps in human cortex. *Journal of Neurophysiology* (2018) doi:10.1152/jn.00059.2018.
9. Bogler, C., Bode, S. & Haynes, J.-D. Decoding Successive Computational Stages of Saliency Processing. *Current Biology* **21**, 1667–1671 (2011).
10. Saproo, S. & Serences, J. T. Spatial Attention Improves the Quality of Population Codes in Human Visual Cortex. *Journal of Neurophysiology* **104**, 885–895 (2010).
11. Serences, J. T. & Yantis, S. Spatially Selective Representations of Voluntary and Stimulus-Driven Attentional Priority in Human Occipital, Parietal, and Frontal Cortex. *Cerebral Cortex* **17**, 284–293 (2007).
12. Bisley, J. W. & Mirpour, K. The neural instantiation of a priority map. *Current Opinion in Psychology* **29**, 108–112 (2019).
13. Theeuwes, J. Goal-driven, stimulus-driven, and history-driven selection. *Current Opinion in Psychology* **29**, 97–101 (2019).
14. Ipata, A. E., Gee, A. L., Gottlieb, J., Bisley, J. W. & Goldberg, M. E. LIP responses to a popout stimulus are reduced if it is overtly ignored. *Nature Neuroscience* **9**, 1071–1076 (2006).
15. Ipata, A. E., Gee, A. L., Bisley, J. W. & Goldberg, M. E. Neurons in the lateral intraparietal area create a priority map by the combination of disparate signals. *Experimental Brain Research* **192**, 479–488 (2009).
16. Geng, J. J., Won, B.-Y. & Carlisle, N. B. Distractor Ignoring: Strategies, Learning, and Passive Filtering. *Curr Dir Psychol Sci* **28**, 600–606 (2019).
17. Le Pelley, M. E., Mitchell, C. J., Beesley, T., George, D. N. & Wills, A. J. Attention and associative learning in humans: An integrative review. *Psychological Bulletin* **142**, 1111–1140 (2016).

18. Van Moorselaar, D. & Slagter, H. A. Inhibition in selective attention. *Annals of the New York Academy of Sciences* **1464**, 204–221 (2020).
19. Mazer, J. A. & Gallant, J. L. Goal-Related Activity in V4 during Free Viewing Visual Search. *Neuron* **40**, 1241–1250 (2003).
20. Poltoratski, S., Ling, S., McCormack, D. & Tong, F. Characterizing the effects of feature salience and top-down attention in the early visual system. *Journal of Neurophysiology* **118**, 564–573 (2017).
21. Gandhi, S. P., Heeger, D. J. & Boynton, G. M. Spatial attention affects brain activity in human primary visual cortex. *Proceedings of the National Academy of Sciences* **96**, 3314–3319 (1999).
22. Somers, D. C., Dale, A. M., Seiffert, A. E. & Tootell, R. B. H. Functional MRI reveals spatially specific attentional modulation in human primary visual cortex. *Proceedings of the National Academy of Sciences* **96**, 1663–1668 (1999).
23. Motter, B. C. Focal attention produces spatially selective processing in visual cortical areas V1, V2, and V4 in the presence of competing stimuli. *Journal of Neurophysiology* **70**, 909–919 (1993).
24. Tootell, R. B. H. *et al.* The Retinotopy of Visual Spatial Attention. *Neuron* **21**, 1409–1422 (1998).
25. Ogawa, T. & Komatsu, H. Neuronal dynamics of bottom-up and top-down processes in area V4 of macaque monkeys performing a visual search. *Exp Brain Res* **173**, 1–13 (2006).
26. Zhang, X., Zhaoping, L., Zhou, T. & Fang, F. Neural Activities in V1 Create a Bottom-Up Saliency Map. *Neuron* **73**, 183–192 (2012).
27. Li, Z. A saliency map in primary visual cortex. *Trends in Cognitive Sciences* **6**, 9–16 (2002).
28. Beck, V. M., Hollingworth, A. & Luck, S. J. Simultaneous Control of Attention by Multiple Working Memory Representations. *Psychol Sci* **23**, 887–898 (2012).
29. Olivers, C. N. L., Meijer, F. & Theeuwes, J. Feature-based memory-driven attentional capture: Visual working memory content affects visual attention. *Journal of Experimental Psychology: Human Perception and Performance* **32**, 1243–1265 (2006).
30. Carlisle, N. B., Arita, J. T., Pardo, D. & Woodman, G. F. Attentional Templates in Visual Working Memory. *Journal of Neuroscience* **31**, 9315–9322 (2011).
31. Pashler, H. & Shiu, L. Do images involuntarily trigger search? A test of Pillsbury's hypothesis. *Psychonomic Bulletin & Review* **6**, 445–448 (1999).
32. Downing, P. E. Interactions Between Visual Working Memory and Selective Attention. *Psychol Sci* **11**, 467–473 (2000).
33. Soto, D., Heinke, D., Humphreys, G. W. & Blanco, M. J. Early, Involuntary Top-Down Guidance of Attention From Working Memory. *Journal of Experimental Psychology: Human Perception and Performance* **31**, 248–261 (2005).
34. Arita, J. T., Carlisle, N. B. & Woodman, G. F. Templates for rejection: Configuring attention to ignore task-irrelevant features. *Journal of Experimental Psychology: Human Perception and Performance* **38**, 580–584 (2012).
35. Conci, M., Deichsel, C., Müller, H. J. & Töllner, T. Feature guidance by negative attentional templates depends on search difficulty. *Visual Cognition* **27**, 317–326 (2019).
36. Moher, J. & Egeth, H. E. The ignoring paradox: Cueing distractor features leads first to selection, then to inhibition of to-be-ignored items. *Attention, Perception, & Psychophysics* **74**, 1590–1605 (2012).
37. Reeder, R. R., Olivers, C. N. L. & Pollmann, S. Cortical evidence for negative search templates. *Visual Cognition* **25**, 278–290 (2017).
38. Beck, V. M. & Hollingworth, A. Evidence for negative feature guidance in visual search is explained by spatial recoding. *Journal of Experimental Psychology: Human Perception and Performance* **41**, 1190–1196 (2015).
39. Becker, M. W., Hemsteger, S. & Peltier, C. No templates for rejection: a failure to configure attention to ignore task-irrelevant features. *Visual Cognition* **23**, 1150–1167 (2015).
40. Failing, M., Feldmann-Wüstefeld, T., Wang, B., Olivers, C. & Theeuwes, J. Statistical regularities induce spatial as well as feature-specific suppression. *Journal of Experimental Psychology: Human Perception and Performance* **45**, 1291–1303 (2019).
41. Wang, B. & Theeuwes, J. Statistical regularities modulate attentional capture. *Journal of Experimental Psychology: Human Perception and Performance* **44**, 13–17 (2018).

42. Won, B.-Y. & Geng, J. J. Passive exposure attenuates distraction during visual search. *Journal of Experimental Psychology: General* (2020) doi:10.1037/xge0000760.
43. Turatto, M. & Pascucci, D. Short-term and long-term plasticity in the visual-attention system: Evidence from habituation of attentional capture. *Neurobiology of Learning and Memory* **130**, 159–169 (2016).
44. Turatto, M., Bonetti, F., Pascucci, D. & Chelazzi, L. Desensitizing the attention system to distraction while idling: A new latent learning phenomenon in the visual attention domain. *Journal of Experimental Psychology: General* **147**, 1827–1850 (2018).
45. Engel, S. A. & Furmanski, C. S. Selective Adaptation to Color Contrast in Human Primary Visual Cortex. *J. Neurosci.* **21**, 3949–3954 (2001).
46. Gardner, J. L. *et al.* Contrast Adaptation and Representation in Human Early Visual Cortex. *Neuron* **47**, 607–620 (2005).
47. Kristjansson, A., Vuilleumier, P., Schwartz, S., Macaluso, E. & Driver, J. Neural Basis for Priming of Pop-Out during Visual Search Revealed with fMRI. *Cerebral Cortex* **17**, 1612–1624 (2007).
48. Grill-Spector, K. & Malach, R. fMR-adaptation: a tool for studying the functional properties of human cortical neurons. *Acta Psychologica* **107**, 293–321 (2001).
49. Failing, M., Wang, B. & Theeuwes, J. Spatial suppression due to statistical regularities is driven by distractor suppression not by target activation. *Atten Percept Psychophys* **81**, 1405–1414 (2019).
50. Geyer, T., Müller, H. J. & Krummenacher, J. Cross-trial priming in visual search for singleton conjunction targets: Role of repeated target and distractor features. *Perception & Psychophysics* **68**, 736–749 (2006).
51. Won, B.-Y., Forloines, M., Zhou, Z. & Geng, J. J. Changes in visual cortical processing attenuate singleton distraction during visual search. *Cortex* (in press).
52. van Moorselaar, D. & Slagter, H. A. Learning What Is Irrelevant or Relevant: Expectations Facilitate Distractor Inhibition and Target Facilitation through Distinct Neural Mechanisms. *J. Neurosci.* **39**, 6953–6967 (2019).
53. Turk-Browne, N. B., Scholl, B. J., Chun, M. M. & Johnson, M. K. Neural Evidence of Statistical Learning: Efficient Detection of Visual Regularities Without Awareness. *Journal of Cognitive Neuroscience* **21**, 1934–1945 (2009).
54. Schapiro, A. C., Gregory, E., Landau, B., McCloskey, M. & Turk-Browne, N. B. The Necessity of the Medial Temporal Lobe for Statistical Learning. *Journal of Cognitive Neuroscience* **26**, 1736–1747 (2014).
55. Theeuwes, J. Perceptual selectivity for color and form. *Perception & Psychophysics* **51**, 599–606 (1992).
56. Gaspelin, N., Leonard, C. J. & Luck, S. J. Direct Evidence for Active Suppression of Salient-but-Irrelevant Sensory Inputs. *Psychol Sci* **26**, 1740–1750 (2015).
57. Gaspelin, N., Leonard, C. J. & Luck, S. J. Suppression of overt attentional capture by salient-but-irrelevant color singletons. *Attention, Perception, & Psychophysics* **79**, 45–62 (2017).
58. Vatterott, D. B. & Vecera, S. P. Experience-dependent attentional tuning of distractor rejection. *Psychon Bull Rev* **19**, 871–878 (2012).
59. Goschy, H., Bakos, S., MÃ¼ller, H. J. & Zehetleitner, M. Probability cueing of distractor locations: both intertrial facilitation and statistical learning mediate interference reduction. *Front. Psychol.* **5**, (2014).
60. Turatto, M. & Galfano, G. Attentional capture by color without any relevant attentional set. *Perception & Psychophysics* **63**, 286–297 (2001).
61. Mounts, J. R. W. Evidence for suppressive mechanisms in attentional selection: Feature singletons produce inhibitory surrounds. *Perception & Psychophysics* **62**, 969–983 (2000).
62. Kamitani, Y. & Tong, F. Decoding the visual and subjective contents of the human brain. *Nat Neurosci* **8**, 679–685 (2005).
63. Serences, J. T. & Saproo, S. Computational advances towards linking BOLD and behavior. *Neuropsychologia* **50**, 435–446 (2012).
64. Norman, K. A., Polyn, S. M., Detre, G. J. & Haxby, J. V. Beyond mind-reading: multi-voxel pattern analysis of fMRI data. *Trends in Cognitive Sciences* **10**, 424–430 (2006).

65. Tong, F. & Pratte, M. S. Decoding Patterns of Human Brain Activity. *Annu. Rev. Psychol.* **63**, 483–509 (2012).
66. Cox, D. D. & Savoy, R. L. Functional magnetic resonance imaging (fMRI) "brain reading": detecting and classifying distributed patterns of fMRI activity in human visual cortex. *NeuroImage* **19**, 261–270 (2003).
67. Haynes, J.-D. & Rees, G. Predicting the orientation of invisible stimuli from activity in human primary visual cortex. *Nat Neurosci* **8**, 686–691 (2005).
68. Emrich, S. M., Riggall, A. C., LaRocque, J. J. & Postle, B. R. Distributed Patterns of Activity in Sensory Cortex Reflect the Precision of Multiple Items Maintained in Visual Short-Term Memory. *Journal of Neuroscience* **33**, 6516–6523 (2013).
69. Lewis-Peacock, J. A. & Postle, B. R. Decoding the internal focus of attention. *Neuropsychologia* **50**, 470–478 (2012).
70. Sprague, T. C., Boynton, G. M. & Serences, J. T. The Importance of Considering Model Choices When Interpreting Results in Computational Neuroimaging. *eNeuro* **6**, ENEURO.0196-19.2019 (2019).
71. Sprague, T. C. *et al.* Inverted Encoding Models Assay Population-Level Stimulus Representations, Not Single-Unit Neural Tuning. *eNeuro* **5**, ENEURO.0098-18.2018 (2018).
72. van Bergen, R. S., Ji Ma, W., Pratte, M. S. & Jehee, J. F. M. Sensory uncertainty decoded from visual cortex predicts behavior. *Nat Neurosci* **18**, 1728–1730 (2015).
73. van Bergen, R. S. & Jehee, J. F. M. Probabilistic Representation in Human Visual Cortex Reflects Uncertainty in Serial Decisions. *J. Neurosci.* **39**, 8164–8176 (2019).
74. Lawson, C. L. & Hanson, R. J. Chapter 23. in *Solving Least-Squares Problems* (Prentice-Hall, 1974).
75. Carandini, M. & Heeger, D. J. Normalization as a canonical neural computation. *Nat Rev Neurosci* **13**, 51–62 (2012).
76. Solomon, S. G. & Kohn, A. Moving Sensory Adaptation beyond Suppressive Effects in Single Neurons. *Current Biology* **24**, R1012–R1022 (2014).
77. Karni, A. & Sagi, D. Where practice makes perfect in texture discrimination: evidence for primary visual cortex plasticity. *Proceedings of the National Academy of Sciences* **88**, 4966–4970 (1991).
78. Schwartz, S., Maquet, P. & Frith, C. Neural correlates of perceptual learning: A functional MRI study of visual texture discrimination. *Proceedings of the National Academy of Sciences* **99**, 17137–17142 (2002).
79. Jehee, J. F. M., Ling, S., Swisher, J. D., van Bergen, R. S. & Tong, F. Perceptual Learning Selectively Refines Orientation Representations in Early Visual Cortex. *Journal of Neuroscience* **32**, 16747–16753 (2012).
80. Feldmann-Wüstefeld, T. & Schubö, A. Intertrial priming due to distractor repetition is eliminated in homogeneous contexts. *Atten Percept Psychophys* **78**, 1935–1947 (2016).
81. Reavis, E. A., Frank, S. M., Greenlee, M. W. & Tse, P. U. Neural correlates of context-dependent feature conjunction learning in visual search tasks. *Hum Brain Mapp* **37**, 2319–2330 (2016).
82. Sawaki, R. & Luck, S. J. Capture versus suppression of attention by salient singletons: Electrophysiological evidence for an automatic attend-to-me signal. *Attention, Perception, & Psychophysics* **72**, 1455–1470 (2010).
83. Gaspar, J. M. & McDonald, J. J. Suppression of Salient Objects Prevents Distraction in Visual Search. *Journal of Neuroscience* **34**, 5658–5666 (2014).
84. Hickey, C., Di Lollo, V. & McDonald, J. J. Electrophysiological Indices of Target and Distractor Processing in Visual Search. *Journal of Cognitive Neuroscience* **21**, 760–775 (2009).
85. Moher, J., Lakshmanan, B. M., Egeth, H. E. & Ewen, J. B. Inhibition Drives Early Feature-Based Attention. *Psychological Science* **25**, 315–324 (2014).
86. Zhang, W. & Luck, S. J. Feature-based attention modulates feedforward visual processing. *Nat Neurosci* **12**, 24–25 (2009).
87. Serences, J. T., Yantis, S., Culberson, A. & Awh, E. Preparatory Activity in Visual Cortex Indexes Distractor Suppression During Covert Spatial Orienting. *Journal of Neurophysiology* **92**, 3538–3545 (2004).

88. Heuer, A. & Schubö, A. Cueing distraction: electrophysiological evidence for anticipatory active suppression of distractor location. *Psychological Research* (2019) doi:10.1007/s00426-019-01211-4.
89. Hickey, C. & Peelen, M. V. Neural Mechanisms of Incentive Salience in Naturalistic Human Vision. *Neuron* **85**, 512–518 (2015).
90. Itthipuripat, S., Vo, V. A., Sprague, T. C. & Serences, J. T. Value-driven attentional capture enhances distractor representations in early visual cortex. *PLoS Biol* **17**, e3000186 (2019).
91. Kim, H. & Anderson, B. A. Dissociable neural mechanisms underlie value-driven and selection-driven attentional capture. *Brain Research* **1708**, 109–115 (2019).
92. Serences, J. T. Value-Based Modulations in Human Visual Cortex. *Neuron* **60**, 1169–1181 (2008).
93. MacLean, M. H. & Giesbrecht, B. Neural evidence reveals the rapid effects of reward history on selective attention. *Brain Research* **1606**, 86–94 (2015).
94. Stanisor, L., van der Togt, C., Pennartz, C. M. A. & Roelfsema, P. R. A unified selection signal for attention and reward in primary visual cortex. *Proceedings of the National Academy of Sciences* **110**, 9136–9141 (2013).
95. Chelazzi, L. *et al.* Altering Spatial Priority Maps via Reward-Based Learning. *Journal of Neuroscience* **34**, 8594–8604 (2014).
96. Anderson, B. A. & Kim, H. On the relationship between value-driven and stimulus-driven attentional capture. *Atten Percept Psychophys* **81**, 607–613 (2019).
97. Maunsell, J. H. R. Neuronal representations of cognitive state: reward or attention? *Trends in Cognitive Sciences* **8**, 261–265 (2004).
98. Hickey, C. & Peelen, M. V. Reward Selectively Modulates the Lingering Neural Representation of Recently Attended Objects in Natural Scenes. *J. Neurosci.* **37**, 7297–7304 (2017).
99. Kastner, S., Pinsk, M. A., De Weerd, P., Desimone, R. & Ungerleider, L. G. Increased Activity in Human Visual Cortex during Directed Attention in the Absence of Visual Stimulation. *Neuron* **22**, 751–761 (1999).
100. Kastner, S. Mechanisms of Directed Attention in the Human Extrastriate Cortex as Revealed by Functional MRI. *Science* **282**, 108–111 (1998).
101. Foster, J. J., Bsales, E. M., Jaffe, R. J. & Awh, E. Alpha-Band Activity Reveals Spontaneous Representations of Spatial Position in Visual Working Memory. *Current Biology* **27**, 3216-3223.e6 (2017).
102. Maljkovic, V. & Nakayama, K. Priming of pop-out: I. Role of features. *Memory & Cognition* **22**, 657–672 (1994).
103. Foster, J. J., Sutterer, D. W., Serences, J. T., Vogel, E. K. & Awh, E. Alpha-Band Oscillations Enable Spatially and Temporally Resolved Tracking of Covert Spatial Attention. *Psychological Science* **28**, 929–941 (2017).
104. Engel, S. A. *et al.* fMRI of human visual cortex. *Nature* **369**, 525–525 (1994).
105. Swisher, J. D., Halko, M. A., Merabet, L. B., McMains, S. A. & Somers, D. C. Visual Topography of Human Intraparietal Sulcus. *Journal of Neuroscience* **27**, 5326–5337 (2007).
106. Brainard, D. H. The Psychophysics Toolbox. *Spat Vis* **10**, 433–436 (1997).
107. Pelli, D. G. The VideoToolbox software for visual psychophysics: transforming numbers into movies. *Spatial Vision* **10**, 437–442 (1997).
108. Andersson, J. L. R., Skare, S. & Ashburner, J. How to correct susceptibility distortions in spin-echo echo-planar images: application to diffusion tensor imaging. *NeuroImage* **20**, 870–888 (2003).
109. Jenkinson, M., Beckmann, C. F., Behrens, T. E. J., Woolrich, M. W. & Smith, S. M. FSL. *NeuroImage* **62**, 782–790 (2012).
110. Smith, S. M. *et al.* Advances in functional and structural MR image analysis and implementation as FSL. *NeuroImage* **23**, S208–S219 (2004).
111. Rademaker, R. L., Chunharas, C. & Serences, J. T. Coexisting representations of sensory and mnemonic information in human visual cortex. *Nat Neurosci* **22**, 1336–1344 (2019).
112. Dale, A. M., Fischl, B. & Sereno, M. I. Cortical Surface-Based Analysis. *NeuroImage* **9**, 179–194 (1999).
113. Greve, D. N. & Fischl, B. Accurate and robust brain image alignment using boundary-based registration. *NeuroImage* **48**, 63–72 (2009).

912 114. Jenkinson, M. & Smith, S. A global optimisation method for robust affine registration of brain
913 images. *Medical Image Analysis* **5**, 143–156 (2001).
914 115. Jenkinson, M., Bannister, P., Brady, M. & Smith, S. Improved Optimization for the Robust and
915 Accurate Linear Registration and Motion Correction of Brain Images. *NeuroImage* **17**, 825–841
916 (2002).
917 116. Brouwer, G. J. & Heeger, D. J. Decoding and Reconstructing Color from Responses in Human
918 Visual Cortex. *Journal of Neuroscience* **29**, 13992–14003 (2009).
919
920